J. Fluid Mech. (1991), *vol.* 229, *pp.* 603–628
Printed in Great Britain

Resonant generation of finite-amplitude waves by the flow of a uniformly stratified fluid over topography

By ROGER GRIMSHAW[1] AND YI ZENGXIN[2]

[1] School of Mathematics, University of New South Wales, Australia

[2] National Research Centre for Marine Environment Forecasts, Hai Dian Division, Beijing, China

(Received 17 May 1990 and in revised form 17 February 1991)

The forced Korteweg–de Vries equation is now established as the canonical equation to describe resonant, or critical, flow over topography. However, when the fluid is uniformly and weakly stratified, this equation degenerates in that the quadratic nonlinear term is absent. This anomalous, but important, case requires an alternative theory which is the purpose of this paper. We derive a new evolution equation to describe this case which, while having some similarities to the forced Korteweg–de Vries equation, contains two important differences. First, a topography of amplitude α now produces a finite-amplitude response, whereas in the canonical forced Korteweg–de Vries equation, the response scales with $\alpha^{\frac{1}{3}}$. Secondly, the maximum amplitude the fluid flow response can achieve is limited by wave breaking, whose onset is characterized by an incipient flow reversal. Various numerical solutions of the new evolution equation are presented spanning a parameter space defined by a resonance detuning parameter, the topographic amplitude and a parameter measuring the strength of the stratification.

1. Introduction

Recently it has been established that the forced Korteweg–de Vries equation (fKdV),

$$-\frac{1}{c_n}(A_\tau+\Delta A_X)+\mu A A_X+\lambda A_{XXX}+\gamma f_X=0, \tag{1.1}$$

is the canonical equation to describe resonant, or critical, flow over topography in a variety of physical situations (see, for instance, Akylas 1984; Cole 1985; Wu 1987; Lee *et al.* 1989 for free-surface flow over an obstacle; Grimshaw & Smyth 1986; Melville & Helfrich 1987 for flow of a stratified fluid over an obstacle; Grimshaw 1990 for flow of a rotating fluid past an obstacle; Grimshaw 1987; Mitsudera & Grimshaw 1990 for flow of a coastal current past a longshore topographic feature). The situations which lead to (1.1) arise when the fluid provides a one-dimensional waveguide and the oncoming flow encounters an obstacle placed transverse to the flow, with the upstream flow speed being close to critical in the sense that the flow speed is close to the linear long-wave phase speed of some wave mode. More specifically, $\alpha^{\frac{1}{3}}A(X,\tau)$ is the amplitude of the dominant, resonant mode, c_n is the linear long-wave phase speed of this mode, $\alpha^{\frac{1}{3}}\Delta$ is the difference between the upstream speed V and c_n so that $\Delta \gtrless 0$ defines supercritical or subcritical flow respectively, $\alpha f(X)$ represents the topography, and μ, λ and γ are coefficients determined by the

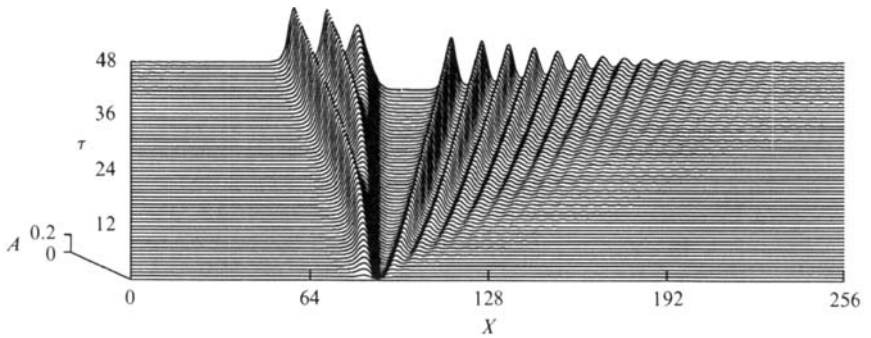

FIGURE 1. A typical numerical solution of the fKdV equation (1.1) with $c_n = 1$, $\Delta = 0$, $\mu = 6$, $\lambda = 1$ and the forcing given by (4.4) with $f_0 = 0.1$, $X_0 = 85$ and $\eta = 0.3$.

particular resonant wave mode being considered; $X = \epsilon x$ is a scaled spatial variable along the waveguide, and $\tau = \alpha^{\frac{1}{2}}\epsilon t$ is a scaled time variable. Here α and ϵ are small parameters where α measures the amplitude of the topography, and ϵ measures the effects of linear dispersion. To obtain the fKdV equation (1.1) the usual KdV-balance $\alpha^{\frac{1}{2}} = \epsilon^2$ is used. Thus (1.1) describes a balance between time evolution, resonant detuning, nonlinearity, wave dispersion and topographic forcing. Note that at resonance a forcing which scales with α produces a response which scales with $\alpha^{\frac{1}{2}}$.

Grimshaw & Smyth (1986) (hereinafter referred to as GS) give a comprehensive account of the solutions of (1.1), obtained numerically and analysed using a combination of modulation theory and hydraulic concepts. The solutions depend mainly on three parameters which are Δ, the detuning parameter, and two other parameters describing the amplitude and width of the forcing term. A typical solution at exact resonance ($\Delta = 0$) is shown in figure 1. It is characterized by an upstream wavetrain of solitary-like waves, a stationary depression in the lee of the obstacle and a downstream modulated wavetrain. These features have been seen in experiments, most noticeably for free-surface flow over an obstacle (e.g. Lee *et al.* 1989), and for two-layer stratified flow over an obstacle (e.g. Baines 1984; Zhu 1986; Melville & Helfrich 1987).

Turning now to the specific case of the flow of a continuously stratified fluid over an obstacle, there have been a number of observations of finite-amplitude long waves propagating upstream (e.g. Wei, Kao & Pao 1975; Baines 1977, 1979; Castro & Snyder 1988; Castro, Snyder & Baines 1990), in qualitative agreement with the predictions of the fKdV equation (1.1). Similar features have been seen in some numerical experiments (e.g. Hanazaki 1989). Often, however, these laboratory and numerical experiments, are conducted for fluids with uniform stratification in the Boussinesq approximation (defined here by requiring the parameter β (2.1) to be small). In this situation the nonlinear coefficient μ in (1.1) vanishes, indicating that the scaling which leads to (1.1) is inappropriate and that the canonical equation (1.1) needs to be altered to describe this situation. Obtaining the appropriate evolution equation for this anomalous, but important case, is the purpose of this paper.

When the coefficient μ vanishes due to a special conjunction of parameters, as occurs, for instance, for a two-layer fluid when both the layer depths and densities are nearly equal, then the remedy is to add a cubic nonlinearity to (1.1) in addition to the small quadratic nonlinearity, thus obtaining a forced modified Korteweg–de Vries equation (e.g. Melville & Helfrich 1987). Here, however, when the coefficient μ vanishes because the fluid is uniformly stratified and the Boussinesq limit is

simultaneously applied, a more drastic remedy is needed. Indeed, for the case to be considered in this paper, the leading-order term in the resonant solution is the product of the amplitude A with the resonant mode, and is an exact solution of the nonlinear, steady, unforced equations. This circumstance is well known in the context of the use of Long's equation to study steady flow over topography, when for a fluid of uniform stratification in the Boussinesq approximation the nonlinear terms vanish identically (see Long **1953**; Yih **1960**; or the Appendix). It now follows that in the evolution equation for this case there are no nonlinear terms of the type seen in (1.1), either quadratic, cubic or any higher order. Instead, the nonlinearity is associated with the time evolution and forcing terms, although we note that if μ is small but not precisely zero, then some traditional nonlinear terms may be present as well.

It follows from this discussion that, if we retain the small parameter α as a measure of the forcing amplitude due to the topography, then the response is of finite amplitude and scales with unity. This should be contrasted with the theory of GS which leads to (1.1) where the response amplitude scales with $\alpha^{\frac{1}{3}}$. Indeed, this observation is perhaps one of the most important conclusions to be drawn from the analysis of this paper. Since here the nonlinearity scales with unity, the evolution equation is determined by a balance between time evolution, resonant detuning, wave dispersion, topographic forcing and perhaps also a parameter measuring the effect of the Boussinesq approximation. We can anticipate that the amplitude of the dominant resonant mode evolves on a timescale of α^{-1} relative to the long-wave timescale, ϵ^{-1}, where ϵ again measures wave dispersion, and hence the appropriate time variable is $\tau = \alpha\epsilon t$. Dispersive effects are proportional to ϵ^2 and we shall adopt the usual KdV balance that $\alpha = \epsilon^2$. The Boussinesq parameter β is also assumed to scale with α. With this scaling we shall derive the required evolution equation (3.25) in §3, and it will be seen that while it belongs to the fKdV family, there are some significant differences from (1.1). In §2 we shall formulate the equations of motion, and give a brief discussion of the linear long-wave theory to provide a background for the subsequent analysis. In §4 we present numerical solutions of the evolution equation (3.26) and compare them with the corresponding solutions of (1.1) described in GS (see figure 1). In §5 we summarize our results. Finally, in the Appendix we reconsider the nonlinear, steady equations with the aim of presenting an alternative view of how the present anomalous case arises.

2. Formulation

We consider the two-dimensional flow of an inviscid, incompressible fluid. Throughout, we shall use non-dimensional variables based on a lengthscale h_1, a typical vertical dimension of the channel, a timescale N_1^{-1} where N_1 is typical of the buoyancy frequency, and a pressure $\rho_1 g h_1$ where ρ_1 is a typical value of the density. These equations define the Boussinesq parameter

$$\beta = \frac{N_1^2 h_1}{g}, \tag{2.1}$$

which we shall assume is small. We shall suppose that the basic state consists of a constant horizontal velocity $V(>0)$, a density $\rho_0(x)$ and a pressure $p_0(z)$ where $p_{0_z} = -\rho_0$. The buoyancy frequency $N(z)$ is defined by

$$\beta\rho_0 N^2 = -\rho_{0_z}. \tag{2.2}$$

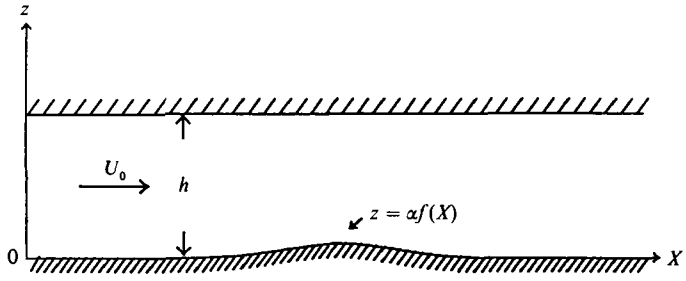

FIGURE 2. The coordinate diagram.

We find it convenient to introduce the vertical particle displacement ζ, so that the density is given by $\rho_0(z-\zeta)$. Then the equations of motion are

$$u_x + w_z = 0, \tag{2.3a}$$

$$\rho_0(z-\zeta)\frac{\mathrm{d}u}{\mathrm{d}t} + p_x = 0, \tag{2.3b}$$

$$\rho_0(z-\zeta)\frac{\mathrm{d}w}{\mathrm{d}t} + p_z + \beta^{-1}\{\rho_0(z-\zeta) - \rho_0(z)\} = 0, \tag{2.3c}$$

$$\frac{\mathrm{d}\zeta}{\mathrm{d}t} - w = 0, \tag{2.3d}$$

where

$$\frac{\mathrm{d}}{\mathrm{d}t} = \frac{\partial}{\partial t} + (V+u)\frac{\partial}{\partial x} + w\frac{\partial}{\partial z}. \tag{2.3e}$$

Here u, w are the velocity components relative to the basic flow, βp is the dynamic pressure and x, z are Eulerian coordinates defining the current position of a fluid particle; in particular, the vertical particle displacement ζ is a function of the current position.

The bottom topography is given by (see figure 2)

$$z = \alpha f(X), \tag{2.4a}$$

where

$$X = \epsilon x. \tag{2.4b}$$

Here α is a small parameter measuring the amplitude of the topography, and ϵ is a second small parameter such that ϵ^{-1} measures the horizontal lengthscale of the topography. We further assume that the topography is localized so that $f \to 0$ as $|X| \to \infty$. The bottom boundary condition is then

$$\zeta = \alpha f \quad \text{at } z = \alpha f. \tag{2.5}$$

If the upper boundary is rigid, then the top boundary condition is

$$\zeta = 0 \quad \text{at } z = h. \tag{2.6}$$

However, if the upper boundary is free with a vertical displacement η, then the top boundary condition is

$$\zeta = \eta \quad \text{at } z = h + \eta, \tag{2.7a}$$

and

$$\beta p = \int_h^{h+\eta} \rho_0(z)\,\mathrm{d}z \quad \text{at } z = h + \eta. \tag{2.7b}$$

For initial conditions we shall suppose that all perturbation variables are zero at $t = 0$. This corresponds, in a frame of reference moving with the basic velocity V, to impulsively moving the obstacle with a constant speed $-V$ for $t > 0$, and represents a typical laboratory experiment. Non-impulsive initial conditions were considered in GS but generally make no difference to the asymptotic state for large times.

To simplify the equations we next introduce the streamfunction ψ where

$$u = \psi_z, \quad w = -\psi_x, \tag{2.8}$$

so that (2.3*a*) is identically satisfied. Eliminating the pressure p from (2.3*b*, *c*) then gives the vorticity equation

$$\frac{\mathrm{d}}{\mathrm{d}t}(\nabla^2\psi) - N^2(z-\zeta)\left\{\zeta_x - \beta\left[\zeta_x \frac{\mathrm{d}}{\mathrm{d}t}(\psi_x) - (1-\zeta_z)\frac{\mathrm{d}}{\mathrm{d}t}(\psi_z)\right]\right\} = 0. \tag{2.9}$$

Also (2.3*d*) becomes

$$\frac{\mathrm{d}\zeta}{\mathrm{d}t} + \psi_x = 0. \tag{2.10}$$

Equations (2.9) and (2.10) thus form two coupled equations for ψ and ζ. To complete the specification of the problem we suppose that the stratification is nearly uniform, and put

$$N^2(z) = N_0^2 + \beta M(z), \tag{2.11}$$

where we recall that β is a small parameter.

To describe the linear long-wave approximation for the case of uniform stratification we put

$$\left.\begin{aligned} \psi &= \alpha\psi_0(X, T, z) + \ldots, \\ \zeta &= \alpha\zeta_0(X, T, z) + \ldots, \end{aligned}\right\} \tag{2.12}$$

where $X = \epsilon x$ (see (2.4*b*)) and $T = \epsilon t$. Then in the joint limit $\alpha, \epsilon, \beta \to 0$, equations (2.9) and (2.10) reduce to

$$\left(\frac{\partial}{\partial T} + V\frac{\partial}{\partial X}\right)\psi_{0zz} = N^2\zeta_{0X}, \tag{2.13a}$$

$$\left(\frac{\partial}{\partial T} + V\frac{\partial}{\partial X}\right)\zeta_0 = -\psi_{0X}, \tag{2.13b}$$

while the boundary conditions (2.5) and (2.6) (or (2.7*a*, *b*)) reduce to

$$\zeta_0 = f \quad \text{at } z = 0, \tag{2.14a}$$

$$\zeta_0 = 0 \quad \text{at } z = h. \tag{2.14b}$$

Note that the limit $\beta \to 0$ removes the distinction between the case of a rigid, or free, upper boundary.

The solution for ζ_0 (or equivalently ψ_0) is most readily obtained by seeking a decomposition into linear long-wave modes. The procedure and result in the general case is described in GS, and the outcome is not changed here, so we shall just give an outline. The linear long-wave modes $v_m(z)$, with phase speeds c_m are here given by

$$v_m(z) = \sin(m\pi z/h), \tag{2.15a}$$

$$c_m = N_0 h/m\pi. \tag{2.15b}$$

Then we let

$$\zeta_0 = \sum_{m=1}^{\infty} A_m(X, T)\, v_m(z), \tag{2.16}$$

and find that

$$\frac{1}{c_m^2}\left(\frac{\partial}{\partial T}+V\frac{\partial}{\partial X}\right)^2 A_m = \frac{\partial^2 A_m}{\partial X^2}+\frac{2}{m\pi}\frac{1}{c_m^2}\left(\frac{\partial}{\partial T}+V\frac{\partial}{\partial X}\right)^2 f. \tag{2.17}$$

With zero initial conditions the solution is (see GS, after correcting some minor errors there)

$$\tfrac{1}{2}m\pi A_m = \frac{V^2}{V^2-c_m^2}f(X)+\frac{c_m}{2(V+c_m)}f(X-[V+c_m]T)-\frac{c_m}{2(V-c_m)}f(x-[V-c_m]T). \tag{2.18}$$

The solution consists of three parts, a steady response over the obstacle, and two waves which propagate at speeds $\pm c_m$ relative to the basic velocity V. If $V > c_m$ both these waves are found downstream, and the flow is supercritical for this mode, but if $V < c_m$ one mode is found upstream and one downstream, and the flow is subcritical for this mode. If $V = c_m$, the flow is critical, or *resonant*, with respect to this mode, the solution (2.18) fails and must be replaced by

$$\tfrac{1}{2}m\pi A_m = \tfrac{1}{2}Vf_X(X)\,T+\tfrac{1}{4}f(X-2VT)+\tfrac{3}{4}f(X). \tag{2.19}$$

The first term is secular as $T\to\infty$ and indicates the necessity for a different theory at resonance.

Before proceeding to examine the resonant theory in the next section, it is of interest to extract the steady part of the solution in (2.18) and then evaluate the corresponding complete steady component from (2.16). We find that

$$\zeta_0 = f(X)\frac{\sin(\pi K[1-z/h])}{\sin(\pi K)}, \tag{2.20a}$$

where

$$K = N_0 h/\pi V. \tag{2.20b}$$

Of course this steady solution can be readily constructed directly from (2.13*a*, *b*). It fails when K is an integer, which of course is just the resonance condition. In the Appendix we show that this method of identifying a resonance from the steady solution can be generalized to non-uniform stratifications.

3. Derivation of the evolution equation

We now suppose that the oncoming flow is resonant with respect to the nth mode and put

$$V = c_n+\alpha\Delta, \tag{3.1}$$

where Δ is a detuning parameter of order unity. As discussed in the introductory section, we anticipate that the amplitude of the dominant resonant mode will evolve on a timescale of α^{-1} relative to the long-wave time variable $T = \epsilon t$, and hence we introduce the slow time variable

$$\tau = \alpha T = \alpha\epsilon t. \tag{3.2}$$

Dispersive effects are proportional to ϵ^2, and we adopt the customary optimal balance $\alpha = \epsilon^2$. Finally, we assume that the Boussinesq parameter β also scales with α, and we put

$$\beta = \sigma\alpha, \tag{3.3}$$

where σ is a parameter of order unity. Then, assuming that ψ and ζ are functions of X, τ and z, equations (2.9) and (2.10) become, after using (2.3e), (2.8) and (2.11),

$$c_n q_X + J(q, \psi) - N_0^2 \zeta_X + \alpha F = 0, \tag{3.4a}$$

$$c_n \zeta_X + J(\zeta, \psi) + \psi_X + \alpha \frac{\mathrm{D}\zeta}{\mathrm{D}\tau} = 0, \tag{3.4b}$$

where

$$\frac{\mathrm{D}}{\mathrm{D}\tau} = \frac{\partial}{\partial \tau} + \Delta \frac{\partial}{\partial X}, \tag{3.4c}$$

$$J(a, b) = a_X b_z - a_z b_X, \tag{3.4d}$$

$$q = \psi_{zz} + \epsilon^2 \psi_{XX}, \tag{3.4e}$$

$$F = \frac{\mathrm{D}q}{\mathrm{D}\tau} - \sigma M(z-\zeta)\zeta_X + \sigma N^2 (z-\zeta)\left[\epsilon^2 \zeta_X \frac{\mathrm{d}}{\mathrm{d}T}(\psi_X) - (1-\zeta_z)\frac{\mathrm{d}}{\mathrm{d}T}(\psi_z)\right], \tag{3.4f}$$

and

$$\frac{\mathrm{d}}{\mathrm{d}T} = c_n \frac{\partial}{\partial X} + J(\cdot, \psi) + \alpha \frac{\mathrm{D}}{\mathrm{D}\tau}. \tag{3.4g}$$

The boundary conditions are (2.5) and (2.6), or (2.7a, b), which we repeat here for convenience

$$\zeta = \alpha f \quad \text{at } z = \alpha f, \tag{3.5a}$$

and

$$\zeta = e\{\sigma \alpha H(1-\zeta_z) + O(\sigma^2 \alpha^2)\} \quad \text{at } z = h, \tag{3.5b}$$

where

$$H_X = \{-c_n \psi_{zX} - J(\psi_z, \psi)\} + O(\alpha). \tag{3.5c}$$

Here $e = 0$ if the upper boundary is rigid, but $e = 1$ if this boundary is free. In the latter case we have used (2.3b) to simplify the boundary condition.

To assist in the integration of (3.4a, b) we introduce the new variable

$$\phi = \psi + c_n z \tag{3.6}$$

and we note that this differs from the total streamfunction $(\psi + Vz)$ only by a term of $O(\alpha)$. Then (3.4a, b) become

$$J\left(q + \frac{N_0^2}{c_n^2}\psi, \phi\right) - N_0^2 \left(\zeta + \frac{\psi}{c_n}\right)_X + \alpha F = 0, \tag{3.7a}$$

$$J\left(\zeta + \frac{\psi}{c_n}, \phi\right) + \alpha \frac{\mathrm{D}\zeta}{\mathrm{D}\tau} = 0. \tag{3.7b}$$

Next we adopt a device used by Warn (1983) (see also Yi & Warn 1987; Grimshaw & Yi 1990) which replaces the vertical coordinate z with ϕ. This is valid provided that

$$\phi_z = \psi_z + c_n \neq 0, \tag{3.8}$$

which is equivalent to requiring that the total horizontal velocity does not vanish, or that the perturbed horizontal velocity is never large enough to cause a flow reversal. We shall see later that the condition (3.8) imposes a restriction on the maximum vertical displacement permitted by this solution procedure. Replacing z with ϕ, (3.7a, b) become

$$\phi_z \left(\frac{\partial}{\partial X}\left[q + \frac{N_0^2}{c_n^2}\psi\right]\right)_\phi - N_0^2 \left(\zeta + \frac{\psi}{c_n}\right)_X + \alpha F = 0, \tag{3.9a}$$

$$\phi_z \left(\frac{\partial}{\partial X}\left[\zeta + \frac{\psi}{c_n}\right]\right)_\phi + \alpha \frac{\mathrm{D}\zeta}{\mathrm{D}\tau} = 0, \tag{3.9b}$$

where the notation $(\partial/\partial X)_\phi$ denotes the derivative with respect to X keeping ϕ constant. Thus (3.9b) implies that

$$\zeta+\frac{\psi}{c_n}=-\alpha\int_{-\infty}^{X}\left(\frac{1}{\phi_z}\frac{\mathrm{D}\zeta}{\mathrm{D}\tau}\right)_{\phi=\text{constant}}\mathrm{d}X'. \tag{3.10}$$

Here, upon integration, an arbitrary function of ϕ should appear on the right-hand side, but considering the upstream limit $X\to-\infty$, we see that this must be zero in the present circumstances. Similarly, on substituting (3.10) into (3.9a), integrating, and using (3.4e) with $\alpha=\epsilon^2$ we obtain

$$\psi_{zz}+\frac{N_0^2}{c_n^2}\psi+\alpha G=0, \tag{3.11a}$$

where

$$G=\psi_{XX}+\int_{-\infty}^{X}\left(\frac{1}{\phi_z}\left\{F+N_0^2\frac{\partial}{\partial X'}\int_{-\infty}^{X'}\left(\frac{1}{\phi_z}\frac{\mathrm{D}\zeta}{\mathrm{D}\tau}\right)_{\phi=\text{constant}}\mathrm{d}X''\right\}\right)_{\phi=\text{constant}}\mathrm{d}X'. \tag{3.11b}$$

Next we expand ζ,ψ as a power series in α,

$$\zeta=\zeta_0(X,\tau,z)+\alpha\zeta_1(X,\tau,z)+\ldots, \tag{3.12a}$$

$$\psi=\psi_0(X,\tau,z)+\alpha\psi_1(X,\tau,z)+\ldots. \tag{3.12b}$$

Substitution into (3.10) and (3.11a) shows that, as discussed in the introductory section, ζ_0 and ψ_0 satisfy linear equations though there is no restriction to infinitesimal amplitudes. Using the boundary conditions (3.5a, b) to leading order, and recalling (2.15b), we find that

$$\zeta_0=-\frac{\psi_0}{c_n}=A(X,\tau)\,v(z), \tag{3.13a}$$

where

$$v(z)=\sin(n\pi z/h). \tag{3.13b}$$

At this state the amplitude $A(X,\tau)$ is undetermined, but consideration of the equation for ψ_1 will yield the desired evolution equation for this amplitude. Indeed, we find from (3.11a) that

$$\psi_{1zz}+\frac{N_0^2}{c_n^2}\psi_1+G_0=0, \tag{3.14}$$

where G_0 is obtained from (3.11b) evaluated to leading order in α. We find that, on using (3.4f), (3.6) and (3.13a, b)

$$\begin{aligned}G_0=&\int_{-\infty}^{X}\left(\frac{v}{1-Av_z}\left\{\frac{N_0^2}{c_n^2}\left(\frac{2-Av_z}{1-Av_z}\right)\frac{\mathrm{D}A}{\mathrm{D}\tau}-\frac{N_0^2}{c_n}\frac{\partial A}{\partial X'}\int_{-\infty}^{X'}\frac{\partial}{\partial\phi}\left(\frac{\dfrac{\mathrm{D}A}{\mathrm{D}\tau}v}{1-Av_z}\right)\mathrm{d}X''\right\}\right)_{\phi=\text{constant}}\mathrm{d}X'\\&-\sigma\int_{-\infty}^{X}\left(\frac{M(z-Av)\,v}{c_n(1-Av_z)}+c_nN_0^2\left(-v_z+\frac{N_0^2}{c_n^2}A\right)\right)_{\phi=\text{constant}}\frac{\partial A}{\partial X'}\mathrm{d}X'\\&-c_nA_{XX}v.\end{aligned} \tag{3.15}$$

The boundary conditions (3.5*a*, *b*) give

$$\psi_1 = -c_n f(1-Av_z) \quad \text{at } z = 0, \tag{3.16a}$$

and

$$\psi_1 = -c_n \sigma e H_0(1-Av_z) \quad \text{at } z = h, \tag{3.16b}$$

where

$$H_0 = c_n^2 v_z A - \tfrac{1}{2}N_0^2 A^2. \tag{3.16c}$$

Equation (3.14) together with the boundary conditions (3.16*a*, *b*) form an inhomogeneous boundary-value problem, which has a solution if and only if the following compatibility condition is satisfied.

$$\int_0^h G_0 v \, \mathrm{d}z - [\psi_1 v_z]_0^h = 0. \tag{3.17}$$

The fact that this condition is necessary follows directly from (3.14) by multiplying (3.14) by v, and integrating with respect to z from 0 to h; after integrating by parts, and recalling the definition of v (3.13*b*), the result (3.17) follows. To show that (3.17) is also sufficient requires solving (3.14) by the method of variation of parameters, and we shall omit the details. On substituting (3.15) and the boundary conditions (3.16*a*, *b*) into (3.17) we obtain an evolution equation for A. The result is considerably simplified if we introduce the variable

$$\xi = z - Av(z), \tag{3.18}$$

where we observe from (3.6) and (3.13*a*), that, to leading order in $\alpha, \phi = c_n \xi$. The relation (3.18) defines $\xi = \xi(z, A)$ whose inverse is $z = z(\xi, A)$, and we recall from (3.8) that the inverse exists if and only if

$$1 - Av_z \neq 0. \tag{3.19}$$

This condition in turn will be satisfied if

$$|A| < h/n\pi = c_n/N_0, \tag{3.20}$$

which is the aforementioned restriction on the maximum vertical displacement permitted. Next we observe that, from (3.18)

$$\frac{\partial z}{\partial A} = \frac{v(z)}{1-Av_z(z)}, \tag{3.21a}$$

and

$$\frac{\partial z}{\partial \xi} = \frac{1}{1-Av_z(z)}. \tag{3.21b}$$

Introducing ξ in place of z in the compatibility condition (3.17), and using the relations (3.21*a*, *b*), we can then show that the evolution equation takes the form

$$-\frac{N_0^2}{c_n^2}\int_{-\infty}^{X} K(A, A')\frac{\mathrm{D}A'}{\mathrm{D}\tau}\,\mathrm{d}X' + \sigma m(A) + \tfrac{1}{2}c_n h A_{XX} + N_0 f\left(1 - \frac{N_0}{c_n}A\right) = 0. \tag{3.22}$$

Here $A' = A(X', \tau)$, while $K(A, A')$ and $m(A)$ are given by

$$K(A, A') = \int_0^h \frac{\partial z}{\partial A}\frac{\partial z'}{\partial A'}\left(1 + \frac{\partial z'}{\partial \xi}\right)\mathrm{d}\xi - \int_0^h (z - z')\frac{\partial z}{\partial A}\frac{\partial}{\partial \xi}\left(\frac{\partial z'}{\partial A'}\right)\mathrm{d}\xi, \tag{3.23a}$$

and

$$m(A) = \frac{1}{c_n}\int_0^h (z-\xi)\frac{\partial z}{\partial A}M(\xi)\,\mathrm{d}\xi + \tfrac{1}{2}N_0^3A^2[1-(-1)^n] - N_0^2c_n\int_0^h \frac{\partial z}{\partial A}\left\{\int_0^A v_z(z')\,\mathrm{d}A'\right\}\mathrm{d}\xi$$
$$-eN_0^2c_n\left(A - \tfrac{3}{2}(-1)^n\frac{N_0}{c_n}A^2 + \frac{1}{2}\frac{N_0^2}{c_n^2}A^3\right). \quad (3.23b)$$

Here $z = z(\xi, A)$ and $z' = z(\xi, A')$. Further, integrating the second term in (3.23a) by parts, it can be shown that $K(A, A')$ is symmetric in A and A', and given by the alternative expression

$$K(A,A') = \int_0^h \frac{\partial z}{\partial A}\frac{\partial z'}{\partial A'}\mathrm{d}\xi - \int_0^h \left\{z\frac{\partial z}{\partial A}\frac{\partial}{\partial \xi}\left(\frac{\partial z'}{\partial A'}\right) + z'\frac{\partial z'}{\partial A'}\frac{\partial}{\partial \xi}\left(\frac{\partial z}{\partial A}\right)\right\}\mathrm{d}\xi. \quad (3.24)$$

Before proceeding in the next section to describe various numerical solutions of (3.22) we record some general properties of (3.22). First it can be shown that

$$\int_{-\infty}^{X} K(A,A')\frac{\partial A'}{\partial X'}\mathrm{d}X' = hA, \quad (3.25)$$

and hence (3.22) adopts the alternative form

$$-\frac{N_0^2}{c_n^2}\int_{-\infty}^{X} K(A,A')\frac{\partial A'}{\partial \tau}\mathrm{d}X' - \frac{hN_0^2}{c_n^2}\Delta A + \sigma m(A) + \tfrac{1}{2}c_n hA_{XX} + N_0 f\left(1 - \frac{N_0 A}{c_n}\right) = 0. \quad (3.26)$$

Next, we consider the weakly nonlinear limit $A \to 0$ for which it can be shown that

$$K(A,A') = h\left\{1 - \frac{1}{4}\frac{N_0^2}{c_n^2}(3A^2 - 8AA' + 3A'^2) + \ldots\right\}. \quad (3.27)$$

Turning now to the nonlinear term $\sigma m(A)$ we first observe that it can be omitted in the limit $\sigma \to 0$, which corresponds to the Boussinesq approximation in which $\beta \ll \alpha$ (see (3.3)). The precise form of $m(A)$ depends on $M(z)$ (see (2.11)), but note that, from (3.26), any linear term in A can be absorbed into a redefinition of Δ, and is equivalent to a β-correction to the phase speed c_n. In analysing $m(A)$ we see from (3.22b) that it can be regarded as composed from three contributions, these being due to $M(z)$, the inertial effects of the stratification, and the free-surface boundary condition, where the last term is identified by the parameter e. First let $M(z) = 0$ corresponding to uniform stratification. Then, in the weakly nonlinear limit $A \to 0$, we find that, putting $e = 0$ for simplicity,

$$m(A) = \tfrac{1}{6}N_0^3A^2[1-(-1)^n] + O(A^4). \quad (3.28)$$

Next let $M(z) = N_0^4 z$, corresponding to an error of $O(\beta^3)$, to the linear stratification $\rho_0(z) = \rho_1(1 - \beta N_0^2 z)$. Then, again using the weakly nonlinear limit and putting $e = 0$, we find that

$$m(A) = \frac{N_0^4 h^2}{4c_n}A - \tfrac{1}{2}N_0^3A^2[1-(-1)^n] + O(A^4). \quad (3.29)$$

Note the curious fact that in both these examples there is no cubic term in A. Recalling that linear terms in A can be absorbed into a redefinition of Δ, we see that a useful approximation to $m(A)$ is a single quadratic term, although the sign of this

term is sensitive to the details of the stratification. Further, we note that in the weakly nonlinear limit (3.26) can be reduced to the fKdV equation (1.1) where $\lambda = c_n^2/2N_0^2$, $\gamma = 1/n\pi$ and the coefficient μ depends on the precise form chosen for $M(z)$, but is proportional to σ.

To conclude, we consider the steady travelling wave solutions of (3.26) in the absence of the forcing term (i.e. $f = 0$). Thus we put $A = A(X - w\tau)$ and using (3.25) we find that

$$\frac{N_0^2}{c_n^2} h(w - \Delta) A + \sigma m(A) + \tfrac{1}{2} c_n h A_{XX} = 0. \tag{3.30}$$

In general this will have both solitary and periodic wave solutions. For instance, if $m(A)$ is a quadratic function of A, $m(A) = 3A^2$ say, then the solitary wave solution of (3.30) is

$$A = a \operatorname{sech}^2 k(X - w\tau), \tag{3.31a}$$

where

$$\Delta - w = \frac{2c_n^2}{N_0^2} \frac{\sigma a}{h} = \frac{2c_n^3}{N_0^2} k^2. \tag{3.31b}$$

Of course, this is just the well-known KdV solitary wave, and this discussion serves to emphasize that the significant new feature of (3.26) resides in the time evolution process described by the first term in (3.26).

4. Solutions of the evolution equation

The equation to be solved is (3.26), where from the discussion at the end of §3, we choose the nonlinear term $m(A)$ to be quadratic, so that

$$m(A) = 3A^2. \tag{4.1}$$

Note that any coefficient of this expression can be absorbed into the definition of the parameter σ. Next we introduce the scaled variables.

$$\tau^* = \frac{c_n^3 \tau}{2N_0^2}, \quad \Delta^* = \frac{2N_0^2 \Delta}{c_n^3}, \quad \sigma^* = \frac{2\sigma}{c_n h}, \quad f^* = \frac{2N_0}{c_n h} f, \tag{4.2}$$

into (3.26). Omitting the asterisk, and using (4.1) the evolution equation to be solved is thus

$$-\frac{1}{h} \int_{-\infty}^{X} K(A, A') \frac{\partial A'}{\partial \tau} \mathrm{d}X' - \Delta A + 3\sigma A^2 + A_{XX} + f\left(1 - \frac{n\pi}{h} A\right) = 0, \tag{4.3}$$

where we recall from (2.15b) that $c_n = N_0 h/n\pi$. Finally we note that there is no loss of generality in setting $h = 1$, since our initial non-dimensionalization was based on the channel depth. The kernel $K(A, A')$ is defined by (3.23a), or equivalently by (3.24). Equation (4.3) contains three intrinsic parameters being the detuning parameter Δ, the nonlinearity parameter σ and the mode number n. In addition there are external parameters associated with the forcing function $f(X)$. To reduce the parameter space we set the mode number $n = 1$, and let the obstacle be a single hump given by

$$f = f_0 \exp(-\eta^2 (X - X_0)^2). \tag{4.4}$$

The forcing function is thus characterized by two parameters f_0 and η, where f_0 is the forcing amplitude and can take either sign, while η^{-1} measures the half-width of the obstacle. Other single hump forcing terms such as a 'sech^2' profile characterized by

the same two parameters will give similar results. The forcing is centred at X_0 which is chosen for numerical convenience; in all the plots shown $X_0 = 85$. To complete the specification of the problem we impose the initial condition that

$$A = 0 \quad \text{at } \tau = 0. \tag{4.5}$$

This corresponds to the laboratory situation in which for times $\tau < 0$ the obstacle and the fluid are at rest, but for times $\tau > 0$ the obstacle is moved at constant speed $-V$. Of course the evolution equation describes this situation from a reference frame attached to the obstacle. Finally we suppose that for all finite times $\tau > 0$, $A \to 0$ as $|X| \to \infty$.

Equation (4.3) with the forcing given by (4.4) and with the initial condition (4.5) was integrated numerically. The numerical scheme is similar to that used by Yi & Warn (1987) and Grimshaw & Yi (1990) for evolution equations of the same type as (4.3), and is described in detail in the former paper. Briefly, as it stands (4.3) can be regarded as a Volterra integral equation of the first kind for the time derivative $\partial A/\partial \tau$. But since the inversion of a first kind integral equation is ill-posed and hence numerically unstable, (4.3) is first differentiated with respect to X to give a Volterra integral equation of the second kind for $\partial A/\partial \tau$ whose inversion is numerically stable. Spatial derivatives are evaluated spectrally over the spatial domain $0 < X < L$, with periodic boundary conditions being applied at $X = 0$, L. The forcing centre X_0, $0 < X_0 < L$ is chosen to maximize the time for the waves generated by the obstacle to reach the domain boundaries, and effectively A is zero at these boundaries until this time is reached.

In presenting our numerical results the available parameters are Δ, σ, f_0 and η. We shall generally set $\eta = 0.3$, since we find the results are relatively insensitive to η; a similar situation was found by GS in the numerical solutions of the fKdV equation (1.1). This leaves the three parameters Δ, σ and f_0 representing respectively the resonance detuning, nonlinearity and the forcing amplitude. Note that although we are calling σ the nonlinearity parameter, it is also a measure of the stratification since the Boussinesq parameter $\beta = \sigma\alpha$ (3.3). Further, there are other nonlinear terms in the kernel $K(A, A')$ and in the total forcing term $f(1 - n\pi A/h)$, and these remain when $\sigma = 0$. In describing our numerical results we shall use as a benchmark the corresponding solutions of the fKdV equation (1.1) described by GS, where we note that a rescaling analogous to (4.2), allows us to set $c_n = 1$, $\mu = 6$, $\lambda = 1$ and $\gamma = 1$ in (1.1). With these values, the weakly nonlinear limit of (4.3) (i.e. $f_0, A \to 0$) is (1.1). It is important to note here that in (1.1) A itself can be rescaled to allow the nonlinear coefficient μ to be chosen arbitrarily, although of course f must also then be rescaled by the same factor. Our choice of $\mu = 6$ for (1.1) corresponds to $\sigma = 1$ in (4.3). Thus in (1.1) there are only two parameters Δ and f_0. However, the corresponding nonlinear parameter σ in (4.3) cannot be removed by an analogous rescaling of A since the kernel $K(A, A')$ and the total forcing term $f(1 - n\pi A/h)$ also depend non-trivially on A.

A typical solution to the fKdV equation (1.1) is shown in figure 1 for the case of positive forcing ($f_0 = 0.1$) and exact resonance ($\Delta = 0$). It is characterized by solitary-like waves, propagating upstream, a stationary depression in the lee of the obstacle and a downstream modulated wavetrain. As Δ is varied, either $\Delta > 0$ (supercritical flow) or $\Delta < 0$ (subcritical flow), there is a resonant band $\Delta_- < \Delta < \Delta_+ (\Delta_\pm \gtrless 0)$ for which the solution retains the same general features. For $\Delta < 0$, the downstream wavetrain intensifies and propagates more slowly until for $\Delta < \Delta_-$ a stationary wavetrain develops in the lee of the obstacle; simultaneously

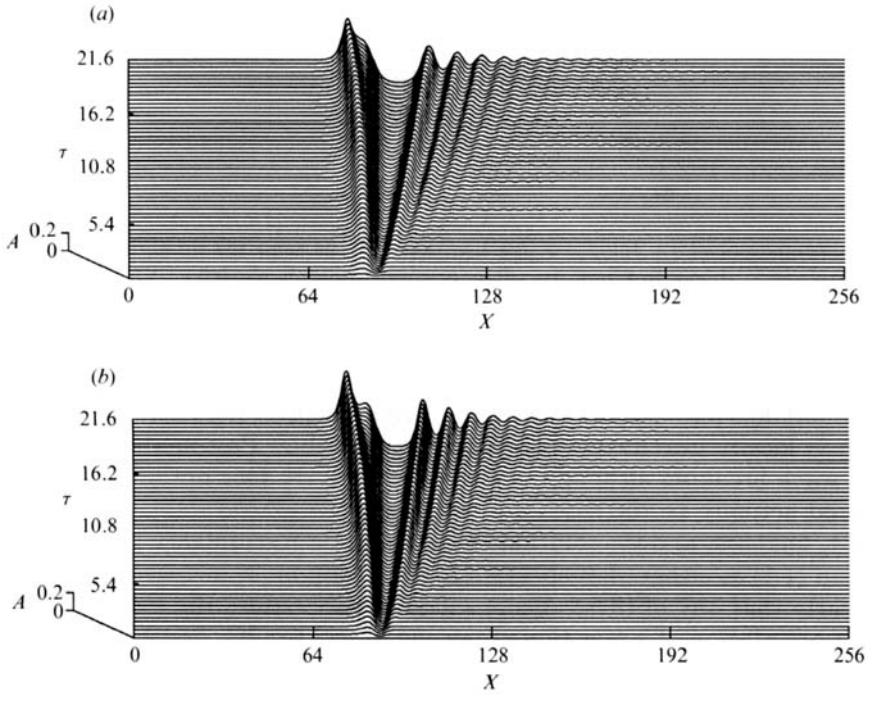

FIGURE 3. (*a*) The numerical solution of (4.3) with $\sigma = 1$, $\Delta = 0$, and $f_0 = 0.1$. Here, and in all the plots shown unless stated otherwise, $X_0 = 85$ and $\eta = 0.3$. (*b*) The corresponding numerical solution of the fKdV equation (1.1).

the upstream wavetrain develops the character of a modulated wavetrain and for $\Delta < \Delta_-$ detaches from the obstacle. On the other hand for $\Delta > 0$, the downstream wavetrain weakens and propagates faster, while the upstream wavetrain slows down, until for $\Delta > \Delta_+$ there develops a stationary elevation over the obstacle and a compensating downstream wavetrain propagating rapidly away from the obstacle. Further details can be found in GS, which also looks at the case of negative forcing $f_0 < 0$.

In general, the solutions of (4.3) show the same qualitative features with some differences which we describe in detail below. First, however, we must emphasize that one of the most important differences is due to the constraint (3.20), which for $h = 1$ and $n = 1$ becomes

$$|A| < \frac{1}{\pi}. \tag{4.6}$$

There is no counterpart to this in the fKdV equation (1.1), which although only valid in the weakly nonlinear limit, in itself places no restriction on the magnitude of A. In many cases we find that even for quite small forcing amplitudes $|f_0|$, the amplitude of the developing wavetrains grows until the constraint (4.6) is violated at some critical time $\tau = \tau_c$. The consequence of this is that the wavetrains do not have time to develop fully, and in particular, we find that the upstream wavetrain often fails to develop and remains confined to the vicinity of the obstacle. It is appropriate here to recall the origin of the constraint (4.6) which is the condition (3.8) preventing a flow reversal at any point in the flow field. Hence we shall call τ_c the breaking time since it corresponds to the time at which the total horizontal velocity has become

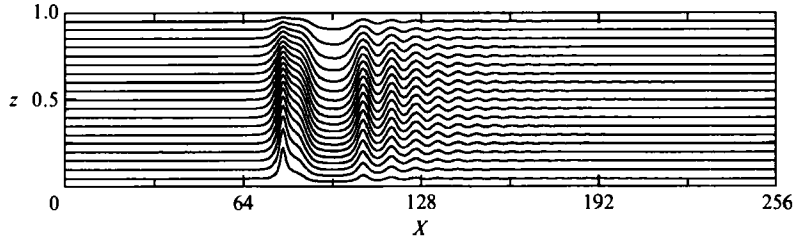

FIGURE 4. A contour plot of $z-Av(z)$ at τ just less than $\tau_c = 21.6$ for the numerical solution of (4.3) shown in figure 3(*a*). The contour intervals are 0.05.

zero at some point in the flow field $X = X_c$, $z = z_c$ say; since $n = 1$ it follows from (3.13*b*) and (3.19) that $z_c = \frac{1}{2}h$. If the wave were allowed to continue for $\tau > \tau_c$ then a situation would develop with heavier fluid overlying lighter fluid leading to a wave profile which is locally gravitationally statically unstable. Presumably this would then lead to wave breaking although our present analysis does not allow us to test that this would actually be the case.

In general τ_c increases and the solutions show a greater resemblance to those of the fKdV equation (1.1) as either $|\Delta|$ increases, $|f_0|$ decreases, or $|\sigma|$ increases. The reason for this is clearly that any of these effects will generally reduce the size of $|A|$. Next we turn to a presentation of a selection of our numerical results, first for $\sigma = 1$, then for $\sigma = -1$, and finally for the important case of very weak stratification when $\sigma = 0$. In each case we consider a range of values of f_0 and Δ.

(*a*) $\sigma = 1$

A typical result is shown in figure 3(*a*) for exact resonance, $\Delta = 0$, and $f_0 = 0.1$. Here we remind the reader that in all the plots displayed, the obstacle is not shown but is centred at $X_0 = 85$, and $\eta = 0.3$ unless otherwise stated. In this case the breaking time $\tau_c = 21.6$, and the wave which breaks is the solitary-like wave forming on the upstream side of the obstacle. A contour plot of the leading term, $c_n(z-Av(z))$, for the total streamfunction ϕ (see (3.6) and (3.13*a*)) is shown in figure 4 for τ just less than τ_c. In order to help interpret the result shown in figure 3(*a*), we show in figure 3(*b*) the corresponding result for the fKdV equation (1.1); of course, this is just the same solution shown in figure 1, but here for clarity of comparison with figure 3(*a*) we only show the solution up to time τ_c. Comparing figures 3(*a*) and 3(*b*) we can see the same qualitative features, namely, the development of an upstream solitary-like wave, a depression in the lee of the obstacle, and a downstream modulated wavetrain. However, there is now the crucial difference that for the evolution equation (4.3) the upstream wave breaks at $\tau = \tau_c$, whereas for the fKdV equation (1.1) there is no such constraint, and the wavetrains continue to develop as shown in figure 1. Also, a closer quantitative comparison between figure 3(*a*, *b*) at identical times τ shows that for the evolution equation (4.3) both the upstream and the downstream waves are of a slightly smaller amplitude, and are slightly displaced in the downstream direction, while the lee depression is also of a slightly smaller magnitude. For $\sigma = 2, 3$ respectively, with the other parameters unchanged, the breaking times are $\tau_c = 22.4$ and 27 respectively, with a corresponding greater development of the wavetrains. On the other hand for $\sigma = 1$ but with f_0 increased to 0.2, the breaking time is $\tau_c = 6.1$.

Next we consider the supercritical case when $\Delta > 0$. Two representative results are shown in figure 5(*a*, *b*) for $\Delta = 0.5$, $f_0 = 0.1$ and $\Delta = 1.0$, $f_0 = 0.2$ respectively.

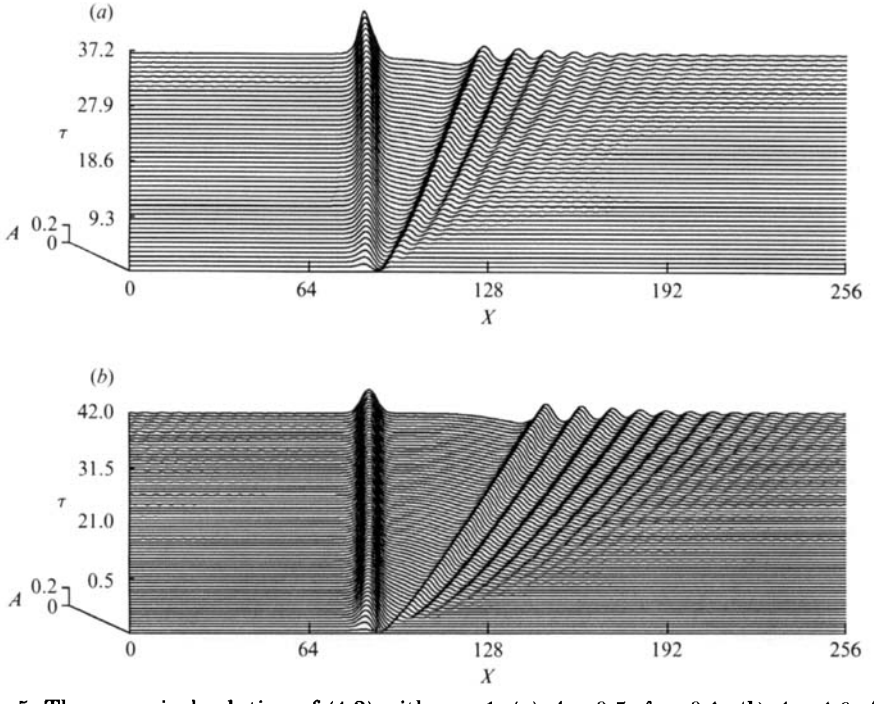

FIGURE 5. The numerical solution of (4.3) with $\sigma = 1$. (*a*) $\Delta = 0.5, f_0 = 0.1$; (*b*) $\Delta = 1.0, f_0 = 0.2$.

Superficially, they appear to be qualitatively similar with a wave of elevation apparently trapped over the obstacle, and a compensating downstream modulated wavetrain. However, there is the important difference that for $\Delta = 0.5$ (figure 5*a*) the wave of elevation is growing slowly and breaks at time $\tau_c = 37.2$, whereas for $\Delta = 1.0$ (figure 5*b*) the wave of elevation is stationary and there is no wave breaking; indeed, this case was run out to $\tau = 82$ with no sign of wave breaking. Comparing these with the analogous results of GS for the fKdV equation (1.1) we would call the case of figure 5(*a*) supercritical but resonant, and the case of figure 5(*b*) supercritical and non-resonant (see figures 7 and 10 of GS). Our interpretation of figure 5(*a*) is that an upstream solitary-like wave is forming but before it is able to detach from the obstacle the breaking time τ_c is reached, whereas in figure 5(*b*) the solution is non-resonant and the waves are too small to break. It is useful here to note that the GS estimate for Δ_+, the upper limit of the resonant band, is $\Delta_+ \approx (12 f_0)^{\frac{1}{2}}$; for the case of figure 5(*a*) this gives $\Delta_+ \approx 1.1$, and for figure 5(*b*) $\Delta_+ \approx 1.55$. Our interpretation of figure 5(*a*) is consistent with these estimates, but for the case of figure 5(*b*) it would seem that there is a residual nonlinear effect in that the evolution equation (4.3) has become non-resonant for a different value of Δ_+ than the fKdV equation (1.1).

For the subcritical cases $\Delta < 0$, three representative results are shown in figure 6(*a*) for $\Delta = -0.4$, $f_0 = 0.1$, figure 6(*b*) for $\Delta = -2.5$, $f_0 = 0.2$ and figure 6(*c*) for $\Delta = -3.0, f_0 = 0.2$. The cases shown in figure 6(*a*, *b*) are resonant in the terminology of GS in that the upstream solitary-like waves are still forming at the obstacle, and the downstream wavetrain is not stationary (see figure 8(*a*) of GS). On the other hand the case shown in figure 6(*c*) is non-resonant since the upstream wavetrain has detached from the obstacle, and there is now a downstream stationary lee-wavetrain (see figure 9 of GS). Note that the GS estimate for Δ_-, the lower limit of the resonant band is $\Delta_- \approx -\frac{1}{2}(12 f_0)^{\frac{1}{2}}$, which is $\Delta_- \approx -0.55$ for the case of figure 6(*a*), and

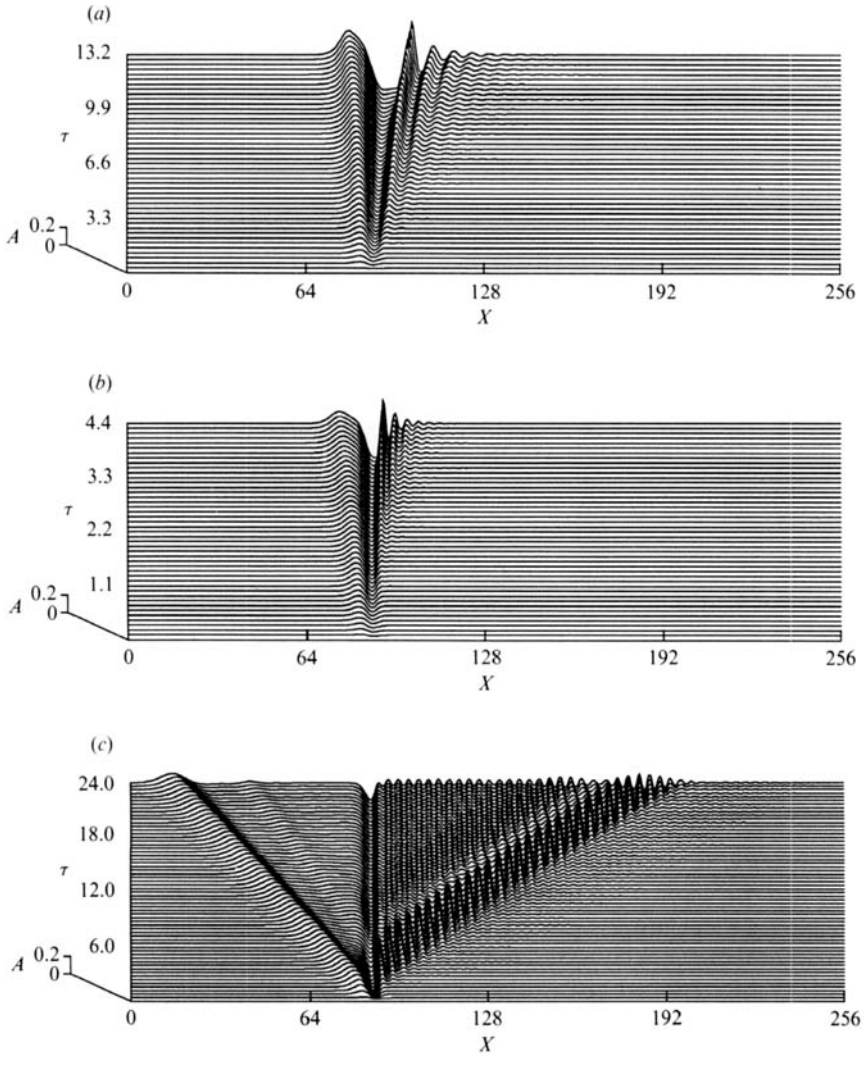

FIGURE 6. The numerical solution of (4.3) with $\sigma = 1$. (*a*) $\Delta = -0.4$, $f_0 = 0.1$; (*b*) $\Delta = -2.5$, $f_0 = 0.2$; (*c*) $\Delta = -3.0$, $f_0 = 0.2$.

$\Delta_- \approx -0.77$ for the cases of figure 6(*b*, *c*). (In fact, GS identify the range $-(12f_0)^{\frac{1}{2}} < \Delta < -\frac{1}{2}(12f_0)^{\frac{1}{2}}$ as a transition band from resonant to fully subcritical, but for simplicity we shall ignore this complication here). However, again, we see that the most significant difference between these results and those of GS is the formation of a breaking wave. Indeed comparing the resonant cases of figure 6(*a*, *b*) with the corresponding result of figure 3(*a*) for $\Delta = 0$, we can see the same qualitative features, although with $\Delta < 0$ the upstream wave has a smaller amplitude, the lee depression is deeper and the downstream waves are larger. Most importantly, breaking now occurs in the lee depression and the breaking time τ_c is reduced as Δ is decreased from zero, being $\tau_c = 13.2$ for $\Delta = -0.4$ (figure 6*a*), 11.4 and 9.9 for $\Delta = -0.5$ and $\Delta = -0.7$, and 4.4 for $\Delta = -2.5$ (figure 6*b*). Further, because of this wave breaking, the boundary between the resonant case and the non-resonant case in the classification scheme of GS is altered here to the criterion that wave breaking

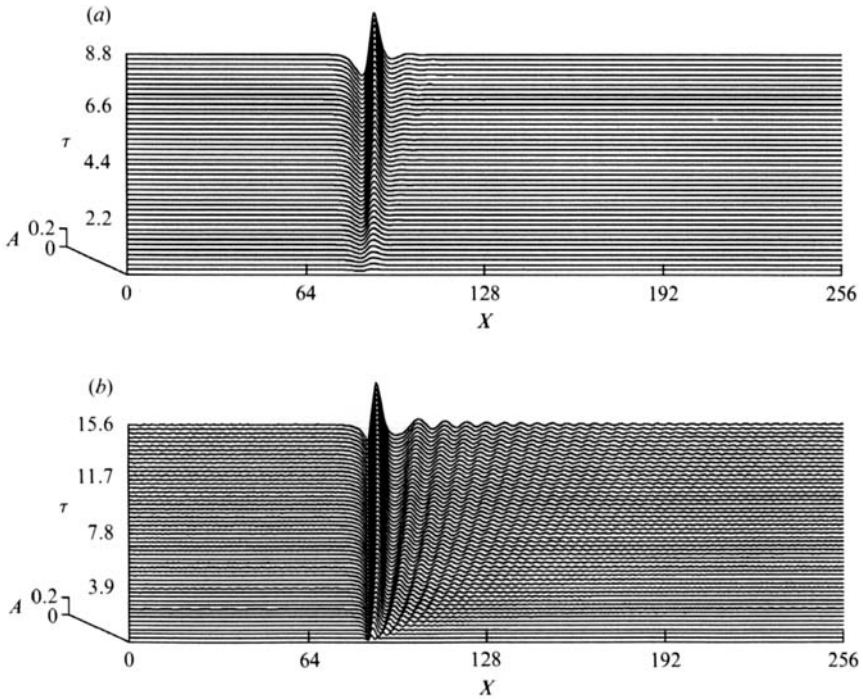

FIGURE 7. The numerical solution of (4.3) with $\sigma = 1$. (*a*) $\Delta = 0, f_0 = -0.1$; (*b*) $\Delta = 0, f_0 = -0.2$ (here $\eta = 2.0$ instead of 0.3).

occurs or does not occur. Finally, comparing the non-resonant case of figure 6(*c*) with the corresponding result (figure 9) of GS, it is interesting to note that although the results are quite similar, here the lee-wavetrain is initially unsteady, and seems to propagate slightly towards the obstacle before becoming steady. Also note that the $O(f_0^2)$ upstream effects predicted by McIntyre (1972) for non-resonant subcritical flow are here too small to be discernible.

Next we consider some representative results for negative forcing ($f_0 < 0$), confining attention to the case of exact resonance. Of course, negative forcing corresponds to flow over a hollow and is of less practical interest than positive forcing, but it is nontheless useful to consider it briefly here in order to give a more complete picture of the solutions of (4.3). With $\Delta = 0$, two typical results are shown in figure 7(*a*) ($f_0 = -0.1, \eta = 0.3$) and 7(*b*) ($f_0 = -0.2, \eta = 2.0$). At first sight it might seem that there are some differences from the corresponding results for the fKdV equation (1.1) (see figure 11 of GS), where there are significant upstream and downstream wavetrains in addition to the transient disturbance in the forcing region. However, the differences are due to the fact that the transient wave in the forcing region breaks before the upstream and downstream wavetrains can develop. This is most marked in figure 7(*a*), where $\tau_c = 8.8$, and only a very small downstream wave can be seen. In figure 7(*b*) the effect of dispersion has been increased by putting $\eta = 2.0$ instead of $\eta = 0.3$, with the consequence that $\tau_c = 15.8$ (note that f_0 is also changed from -0.1 to -0.2), and there is more time for a significant downstream wavetrain to develop.

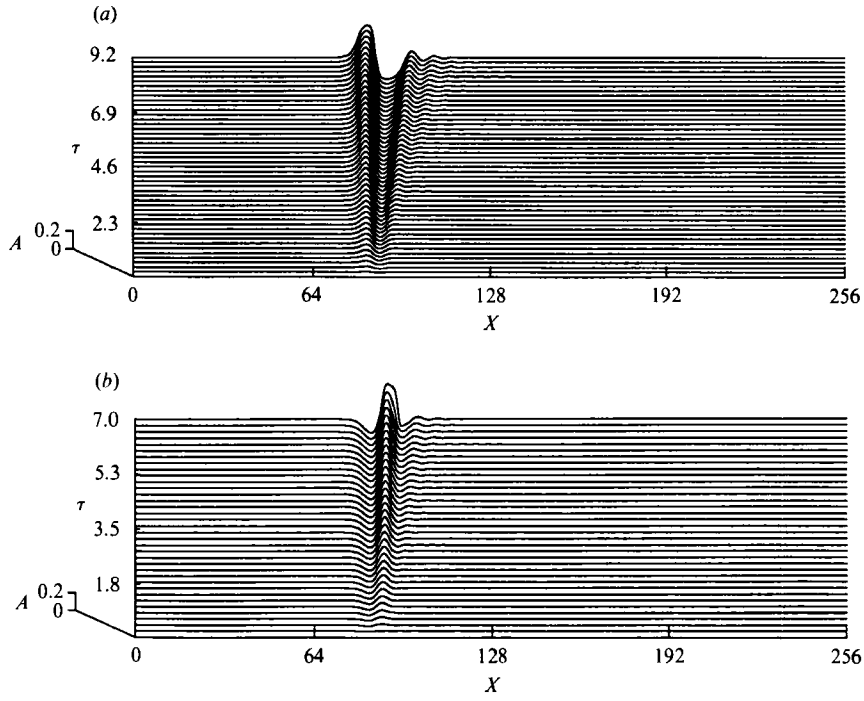

FIGURE 8. The numerical solution of (4.3) with $\sigma = -1$. (*a*) $\Delta = 0, f_0 = -0.1$; (*b*) $\Delta = 0, f_0 = 0.1$. Note that now $-A$ is plotted.

(*b*) $\sigma = -1$

For the fKdV equation (1.1) this case is equivalent to $\sigma = 1$, since the transformation $A \to -A$ and $f \to -f$ is equivalent to changing the sign of the nonlinear coefficient. However, for the evolution equation (4.3) this transformation is not available, and hence $\sigma = -1$ is a distinct case from $\sigma = 1$. Nevertheless, in presenting our results it is useful to keep in mind the transformation $A \to -A$ and $f \to -f$, so that in this subsection our results are plotted for $-A$. In figure 8(*a*, *b*) we show the cases $\Delta = 0$ and $f_0 = -0.1$ and $f_0 = 0.1$ respectively. The case shown in figure 8(*a*) corresponds to that shown in figure 3(*a*) ($\sigma = 1$, $\Delta = 0, f_0 = 0.1$) and we can see the same general features with the important difference that the breaking time has been reduced (from $\tau_c = 21.6$ to $\tau_c = 9.2$). Similarly, the case shown in figure 8(*b*) corresponds to that shown in figure 7(*a*) ($\sigma = 1$, $\Delta = 0, f_0 = -0.1$) and again there are the same general features but with a reduction in the breaking time (now from $\tau_c = 8.8$ to $\tau_c = 7.0$). When $|\Delta| \neq 0$, but remains small, there is a qualitative similarity to the case $\Delta = 0$ with generally similar breaking times; thus for $\Delta = 0.4$ with $f_0 = -0.1$ or $f_0 = 0.1$ we find that $\tau_c = 10.4$ or 12.0 respectively, while for $\Delta = -0.4$ with $f_0 = -0.1$ or $f_0 = 0.1$ we find that $\tau_c = 13.0$ or 6.0 respectively. Generally, as $|\Delta|$ is increased the validity of the comparison with the corresponding case for $\sigma = 1$ under the transformation $A \to -A$ and $f \to -f$ is increased, although as for the case $\Delta = 0$ the corresponding breaking time is generally reduced.

(*c*) $\sigma = 0$

This case is important because the nonlinear terms in (4.3) are entirely associated either with the time evolution term or with the forcing term. In the weakly nonlinear limit it reduces to the linear fKdV equation (i.e. (1.1) with $\mu = 0$). First, we consider

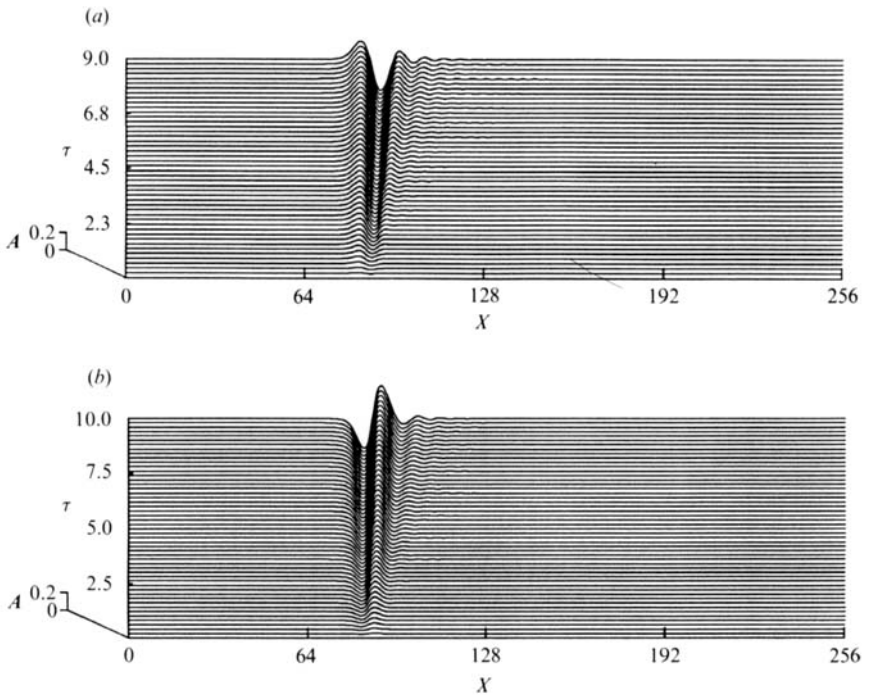

FIGURE 9. The numerical solution of (4.3) with $\sigma = 0$. (*a*) $\Delta = 0, f_0 = 0.1$; (*b*) $\Delta = 0, f_0 = -0.1$.

positive forcing and in figure 9(*a*) show the case of positive forcing ($f_0 = 0.1$) and exact resonance ($\Delta = 0$). There is a qualitative similarity with the corresponding result in figure 3(*a*) for $\sigma = 1$, with the important difference that the breaking time has been substantially reduced from $\tau_c = 21.6$ to $\tau_c = 9.0$, although we note that the corresponding breaking time for $\sigma = -1$ is $\tau_c = 9.2$ (see figure 8*a*). Also, breaking now occurs in the lee depression rather than for the upstream wave. The case of negative forcing ($f_0 = -0.1$) is shown in figure 9(*b*) and the breaking time is now $\tau_c = 10.0$, which is greater than the breaking times $\tau_c = 8.8$ or $\tau_c = 7.0$ for the corresponding cases of $\sigma = 1$ (figure 7*a*) or $\sigma = -1$ (figure 8*b*) respectively.

As Δ or f_0 are varied the comparison with the case $\sigma = 1$ remains useful, but there is generally a reduction in the breaking time. For instance, in figure 10(*a*) we show the case $\Delta = -0.4$, $f_0 = 0.1$ which is subcritical but resonant, and should be compared with the corresponding result for $\sigma = 1$ (figure 6*a*); the breaking time has been reduced from $\tau_c = 13.2$ to $\tau_c = 7.7$ and again occurs in the lee depression. For $\Delta = -0.7$ or -0.9 the breaking time is further reduced to $\tau_c = 7.2$ (in both cases). In figure 10(*b*) we show the case $\Delta = -2.5$, $f_0 = 0.2$ which is subcritical and non-resonant, and should be compared with figure 6(*c*) for the corresponding case of $\sigma = 1$ (see also figure 9 of GS). There is again a stationary lee-wavetrain, and an upstream-propagating wavetrain, but there are some quantitative differences between the cases $\sigma = 0$ and $\sigma = 1$. Most notably, for $\sigma = 0$, the lee-wavetrain remains unsteady for a considerable time before becoming stationary, and the initial propagation towards the obstacle is quite marked. For this case there is no wave breaking up to $\tau = 48$, although for convenience we only show the results up to $\tau = 28$ in figure 10(*b*). However, for $\Delta = -1.5$ and $\Delta = -2.0$ (with $f_0 = 0.2$), wave breaking does occur at $\tau = 34.6$ and $\tau = 37.1$ respectively.

In figure 11(*a*, *b*) we show two supercritical cases, $\Delta = 0.5 (f_0 = 0.1)$ and $\Delta =$

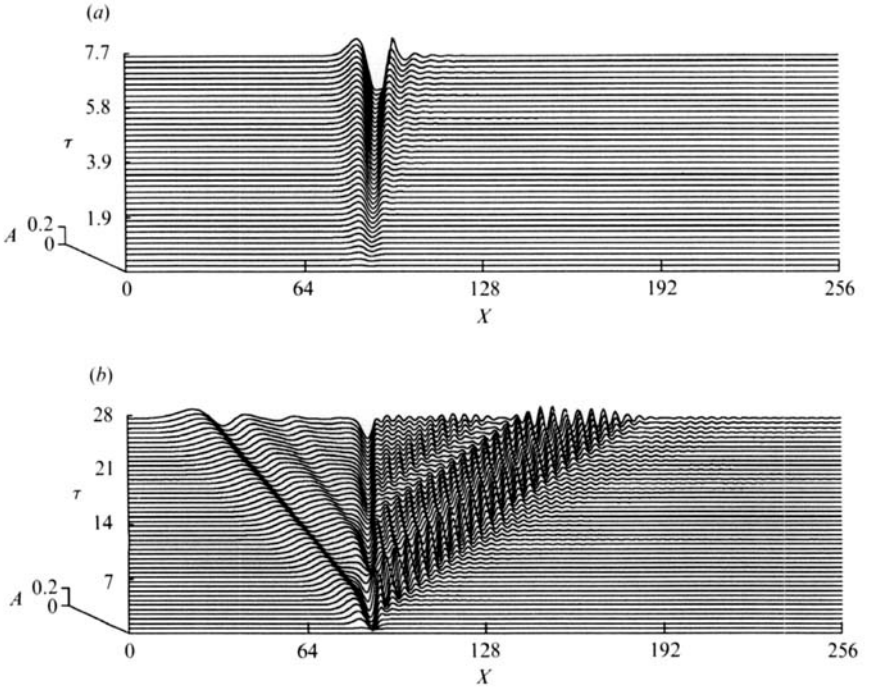

FIGURE 10. The numerical solution of (4.3) with $\sigma = 0$. (*a*) $\Delta = -0.4$, $f_0 = 0.1$; (*b*) $\Delta = -2.5$; $f_0 = 0.2$.

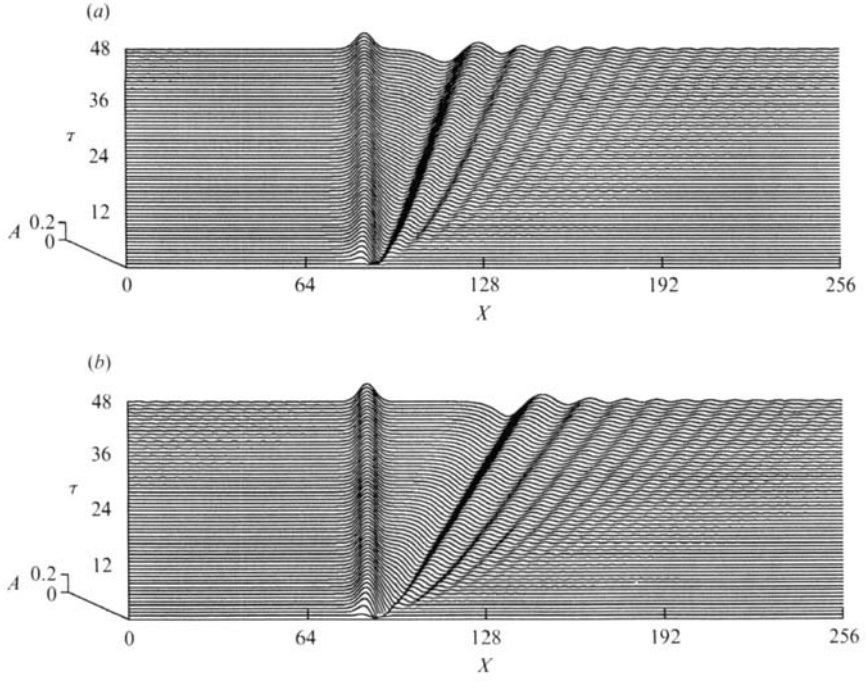

FIGURE 11. The numerical solution of (4.3) with $\sigma = 0$. (*a*) $\Delta = 0.5$, $f_0 = 0.1$; (*b*) $\Delta = 1.0$, $f_0 = 0.2$.

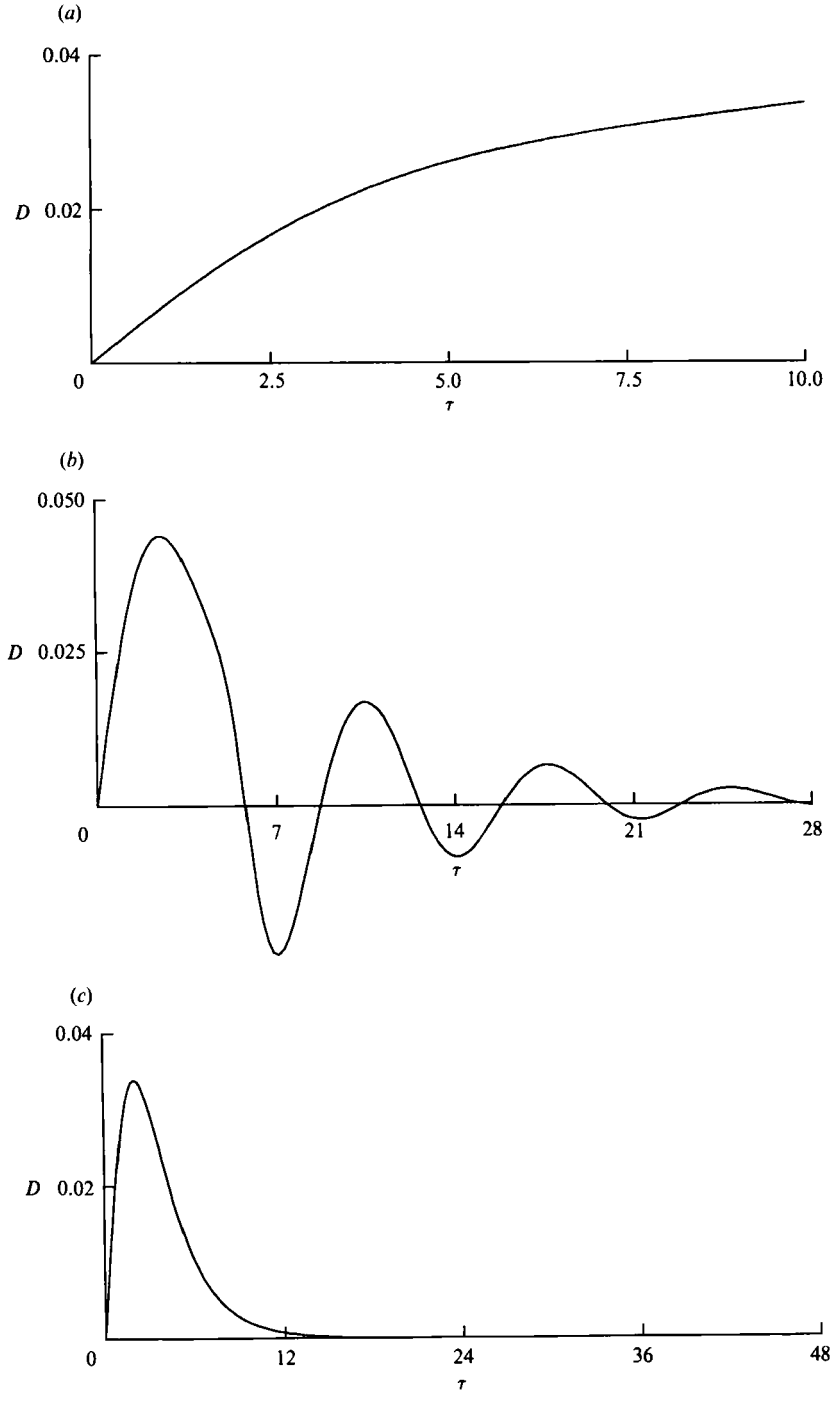

FIGURE 12. The drag D (4.7) for $\sigma = 0$. The plots show $hD/n\pi c_n^2$. (*a*) $\Delta = 0$, $f_0 = 0.1$; (*b*) $\Delta = -2.5$, $f_0 = 0.2$; (*c*) $\Delta = 1.0$, $f_0 = 0.2$. These correspond to figures 9(*a*), 10(*b*) and 11(*b*) respectively.

1.0($f_0 = 0.2$) respectively. In both cases no wave breaking was observed up to $\tau = 48$. However, we classify the case $\Delta = 0.5$ (figure 11*a*) as resonant, since the downstream wavetrain is still connected to the obstacle by a lee depression, while this is not the case for $\Delta = 1.0$ (figure 11*b*) which we hence classify as non-resonant. We note, however, that for $\Delta = 0.5$ and $f_0 = 0.2$ wave breaking occurs at $\tau_c = 5.6$ which should be contrasted with the case $\Delta = 0.5$ and $f_0 = 0.1$ (figure 11*a*) when there is no wave breaking. It is useful to note here that the GS estimate for the resonant band $\Delta_- < \Delta < \Delta_+$ has $\Delta_+ \approx (12 f_0)^{\frac{1}{2}}$ and $\Delta_- \approx -\frac{1}{2}(12 f_0)^{\frac{1}{2}}$; with $f_0 = 0.2$ this gives $\Delta_+ \approx 1.55$ and $\Delta_- \approx -0.77$. It seems that the combination of wave breaking and/or the absence of a traditional nonlinear term (i.e. $\sigma = 0$) makes these estimates only a qualitative guide to the resonant bandwidth.

Finally, because some experiments (e.g. Castro *et al.* 1990) measure the obstacle drag we give three representative results for the drag αD, which to leading order in α, is here given by

$$D = -\frac{n\pi}{h} c_n^2 \int_{-\infty}^{\infty} f A_X \left(1 - \frac{n\pi}{h} A\right) \mathrm{d}X. \tag{4.7}$$

In figure 12(*a*) we show a time history of D for $\Delta = 0$ and $f_0 = 0.1$ (see figure 9(*a*) for the corresponding evolution of A). We see that D increases until breaking occurs, owing to the simultaneous growth of the upstream wave and lee depression. In figure 12(*b*, *c*) we show D for $\Delta = -2.5$ and $\Delta = 1.0$ respectively with $f_0 = 0.2$ (see figures 10(*b*) and 11(*b*) for the corresponding evolution of A). In the subcritical case D oscillates as each successive upstream wave is produced, and presumably eventually decays to a steady value. Oscillations in wave drag for subcritical flow have been observed by Castro *et al.* (1990), although a direct comparison with the experimental results is precluded, *inter alia*, by the neglect of frictional effects in the present theory. In the supercritical case, D rises rapidly as the initial downstream wave forms at the obstacle, but then decays to zero once a steady state is reached over the forcing region.

5. Summary

In this paper we have shown that the canonical fKdV equation (1.1) for resonant flow over topography is replaced by the evolution equation (3.26) (or (4.3) in scaled form) in the important special case when the fluid is uniformly and weakly stratified. While this new evolution equation has solutions which bear some qualitative similarity to those of the fKdV equation there are two important differences. The first is that in the present case, for near resonant flow, a topography whose amplitude scales with the small parameter α, will produce a response amplitude which scales with unity. Secondly, the maximum amplitude which the fluid flow response can achieve is limited by wave breaking, whose onset is here defined as an incipient flow reversal.

In general, the evolution equation (3.26) describes, for resonant (or critical) flow over topography, a fluid response which consists of the development of upstream solitary-like waves, a lee depression on the immediate downstream side of the topography, and a compensating downstream train of modulated waves. Often, particularly for a flow which is near an exact linear resonance, this fluid response produces a breaking wave either on the upstream side of the topography, or in the lee depression. The latter case is more common when the flow is on the subcritical side of resonance. However, if wave breaking does not occur, which is typically the case

when the flow parameters are such that the system is not near an exact linear resonance, then the solutions behave similarly to those of the fKdV equation, and indeed the evolution equation (3.26) reduces to an fKdV equation when the wave amplitudes become small. Further, the similarity to the fKdV equation is enhanced when the conditions of the Boussinesq approximation and uniform stratification are slightly relaxed by increasing the absolute value of the parameter σ in the evolution equation (3.26).

To conclude we have shown that the evolution equation (3.26) replaces the canonical fKdV equation (1.1) in the anomalous, but important, case of uniform stratification in the Boussinesq approximation. The need for this extension of the generic theory is indicated by the fact that the nonlinear coefficient μ in the fKdV equation (1.1) vanishes identically in this special case. Indeed the same anomalous situation occurs in the resonant flow of a rotating fluid past an obstacle when the oncoming flow is uniform with constant angular velocity (Grimshaw 1990), and in that case too the fKdV equation (1.1) is replaced by an evolution equation similar to (3.26). Finally, although the present work was originally motivated by the experiments of Castro *et al.* (1990), a direct comparison with these experiments, or indeed with the earlier experiments of Baines (1979) or the numerical results of Hanazaki (1989), is precluded by the absence of friction in the present theory. We are currently examining a modification of the present model equation which incorporates frictional effects with the major aim of determining to what extent frictional processes can prevent wave breaking.

Yi Zengxin was supported during this project by ARC grant A48830746.

Appendix

Here we shall consider the nonlinear, steady equations with the aim of developing an alternative, but equivalent, criterion for resonance. Hence we now put $\partial/\partial t = 0$ in (2.9) and (2.10). Equation (2.10) then becomes

$$J\left(\zeta+\frac{\psi}{V},\phi\right)=0, \tag{A 1a}$$

where

$$\phi=\psi+Vz. \tag{A 1b}$$

Note that ϕ differs slightly from the definition (3.6) given in §3. Using the upstream condition that $\zeta,\psi\to 0$ as $X\to-\infty$, it follows that

$$\zeta+\frac{\psi}{V}=0. \tag{A 2}$$

Then (2.9) becomes

$$VJ(q,\phi)+N^2\left(\frac{\phi}{V}\right)\{\psi_X-\beta[\epsilon^2\phi_X J(\phi_X,\phi)+\phi_z J(\phi_z,\phi)]\}=0, \tag{A 3}$$

where we recall that q is given by (3.4e). Again using the upstream conditions (A 3) can be integrated to give

$$\psi_{zz}+\alpha\psi_{XX}+N^2\left(\frac{\phi}{V}\right)\left\{\frac{\psi}{V^2}-\frac{\beta}{2V}(\epsilon^2\psi_X^2+\psi_z^2+2V\psi_z)\right\}=0. \tag{A 4}$$

The boundary conditions (2.5) and (2.6) become

$$\psi = -\alpha V f \quad \text{at } z = \alpha f, \tag{A 5a}$$

and

$$\psi = 0 \quad \text{at } z = h. \tag{A 5b}$$

If the upper boundary is free, (2.6) is replaced by (2.7a, b) which become

$$\psi = -V\eta \quad \text{at } z = h+\eta, \tag{A 6a}$$

and

$$\psi = \tfrac{1}{2}\beta V(\epsilon^2\psi_X^2 + \psi_z^2 + 2V\psi_z) \quad \text{at } z = h+\eta. \tag{A 6b}$$

Equation (A 4) with the boundary conditions (A 5b) (or (A 5a) and (A 6a, b)) forms a single, nonlinear equation for ψ. Of course, this equation is well known (see, for instance, Long 1953, or Yih 1960), and is often called Long's equation. It has been mainly utilized for the case of uniform stratification in the Boussinesq limit $\beta \to 0$, when it reduces to a linear equation. This case is also the focus of this paper, and we shall discuss this situation below (see the last paragraph). First, however, we consider the general case when $N^2(z)$ is an arbitrary, generally nonlinear function of z, and β is not necessarily a small parameter.

At this point we make the long-wave approximation and omit the ϵ^2-terms in (A 4) (and in (A 6b)), so that the equation to be solved is

$$\psi_{zz} + N^2\left(\frac{\phi}{V}\right)\left\{\frac{\psi}{V^2} - \frac{\beta}{2V}(\psi_z^2 + 2V\psi_z)\right\} = 0. \tag{A 7}$$

The X-dependence of the forcing provided by the obstacle is now purely parametric, and (A 7) is to be solved as a second-order ordinary differential equation in z alone. Let $\psi(z; d(X))$ be the solution satisfying the boundary condition (A 5b) or (A 6a, b)); as the notation indicates it depends on a single 'constant of integration' $d(X)$ which depends parametrically on X. Then to satisfy the remaining boundary condition (A 5a) we require that

$$\psi(\alpha f(X); d(X)) = -\alpha V f(X). \tag{A 8}$$

This condition determines d in terms of αf uniquely provided that

$$\psi_d(\alpha f(X); d(X)) \neq 0, \tag{A 9}$$

where the notation indicates the derivative with respect to d. The flow is said to be critical if (A 9) is violated, so that

$$\psi_d(\alpha f(X); d(X)) = 0. \tag{A 10}$$

This definition of criticality is just that introduced by Gill (1977) in a different context (see also Pratt & Armi 1987; Grimshaw 1990), and is equivalent to the condition that a long wave has become stationary (i.e. it has a zero phase speed in the frame of reference of the obstacle). Here, as in Grimshaw (1990) which considers an analogous situation for rotating flows, we shall demonstrate this in the limit $\alpha \to 0$, and confirm that this concept of criticality is equivalent to that of resonance defined in GS.

Thus let

$$v(z; d(X)) = \psi_d(z; d(X)). \tag{A 11}$$

Then, differentiating (A 7) we find that

$$v_{zz} + N^2\left(\frac{\phi}{V}\right)\left\{\frac{v}{V^2} - \beta\left(\frac{\psi_z}{V}v_z + v_z\right)\right\} + (N^2)'\left(\frac{\phi}{V}\right)\frac{v}{V}\left\{\frac{\psi}{V^2} - \frac{\beta}{2V}(\psi_z^2 + 2V\psi_z)\right\} = 0. \tag{A 12}$$

The boundary conditions for v at criticality are

$$v = 0 \quad \text{at } z = \alpha f, \tag{A 13a}$$

and

$$v = 0 \quad \text{at } z = h. \tag{A 13b}$$

If the upper boundary is free, (A 13b) is replaced by a different boundary condition obtained by differentiation of (A 6a, b), but for simplicity we shall not give details. In the limit $\alpha \to 0$, $\psi \to 0$, and hence (A 12) and (A 13a, b) become

$$v_{zz} - \beta N^2(z) v_z + \frac{N^2(z)}{V^2} v = 0, \tag{A 14a}$$

and

$$v = 0 \quad \text{at } z = 0, h. \tag{A 14b}$$

Examination of (A 14a, b) shows that this is identical with the equations defining a linear long-wave free mode (see (2.10a–c) of GS), and has a solution if and only if $V = c_n$. Hence, criticality as $\alpha \to 0$ is equivalent to the definition of resonance given by GS. Note that relative to the obstacle, the linear long-wave phase speeds are $V \pm c_n$.

To conclude, we consider the special case of uniform stratification in the Boussinesq limit $\beta \to 0$. Thus $N^2(z)$ is defined by (2.11), and letting $\beta \to 0$ in (A 7) we obtain

$$\psi_{zz} + N_0^2 \frac{\psi}{V^2} = 0, \tag{A 15}$$

while the boundary conditions are (A 5a, b), whether the boundary is rigid or free. The solution which satisfies the boundary condition (A 5b) is

$$\psi(z; d) = d \sin\left\{\frac{N_0}{V}(h - z)\right\}. \tag{A 16}$$

Thus v (A 11) is given by

$$v(z; d) = \sin\left\{\frac{N_0}{V}(h - z)\right\}. \tag{A 17}$$

The parameter d is determined from (A 8) and hence

$$d = -\alpha V f / \sin\left\{\frac{N_0}{V}(h - \alpha f)\right\}. \tag{A 18}$$

Also the condition (A 10) for criticality becomes

$$\sin\left\{\frac{N_0}{V}(h - \alpha f)\right\} = 0, \tag{A 19}$$

which is also immediately apparent from (A 18). In the limit $\alpha \to 0$, this gives $V = c_n$, where here c_n is given by (2.15b). It is significant here that at resonance, d scales with unity as $\alpha \to 0$ the reason being the linearity of (A 15), and the consequent linear dependence of ψ on d (see (A 16)). In contrast, in the general case when ψ is determined by the nonlinear equation (A 7), ψ will depend nonlinearly on d, and at resonance, it can be shown from (A 8) that d is proportional to $\alpha^{\frac{1}{2}}$ as $\alpha \to 0$, which is the characteristic scaling for resonance discussed in GS. This gives an alternative aspect on why the resonant theory described in this paper requires a different treatment from the general theory of GS.

REFERENCES

AKYLAS, T. R. 1984 On the excitation of long nonlinear water waves by a moving pressure distribution. *J. Fluid Mech.* **141**, 455–466.

BAINES, P. G. 1977 Upstream influence and Long's model in stratified flows. *J. Fluid Mech.* **82**, 147–159.

BAINES, P. G. 1979 Observations of stratified flow over two-dimensional obstacles in fluid of finite depth. *Tellus* **31**, 351–371.

BAINES, P. G. 1984 A unified description of two-layer flow over topography. *J. Fluid Mech.* **146**, 127–167.

CASTRO, I. P. & SNYDER, W. H. 1988 Upstream motions in stratified flow. *J. Fluid Mech.* **135**, 261–282.

CASTRO, I. P., SNYDER, W. H. & BAINES, P. G. 1990 Obstacle drag in stratified flow. *Proc. R. Soc.* A **429**, 119–140.

COLE, S. L. 1985 Transient waves produced by flow past a bump. *Wave Motion* **7**, 579–587.

GILL, A. E. 1977 The hydraulics of rotating-channel flow. *J. Fluid Mech.* **80**, 641–671.

GRIMSHAW, R. 1987 Resonant forcing of barotropic coastally trapped waves. *J. Phys. Oceanogr.* **17**, 53–65.

GRIMSHAW, R. 1990 Resonant flow of a rotating fluid past an obstacle: the general case. *Stud. Appl. Maths* **83**, 249–269.

GRIMSHAW, R. & SMYTH, N. 1986 Resonant flow of a stratified fluid over topography. *J. Fluid Mech.* **169**, 429–464.

GRIMSHAW, R. & YI ZENGXIN 1990 Finite-amplitude long waves on coastal currents. *J. Phys. Oceanogr.* **20**, 3–18.

HANAZAKI, H. 1989 Upstream advancing columnar disturbances in two-dimensional stratified flow of finite depth. *Phys. Fluids* A **1**, 1976–1987.

LEE, S.-J., YATES, G. T. & WU, T. Y. 1989 Experiments and analyses of upstream-advancing solitary waves generated by moving disturbances. *J. Fluid Mech.* **199**, 569–593.

LONG, R. R. 1953 Some aspects of the flow of stratified fluids. I. A theoretical investigation. *Tellus* **5**, 42–57.

MCINTYRE, M. E. 1972 On Long's hypothesis of no upstream influence in uniformly stratified or rotating flow. *J. Fluid Mech.* **52**, 209–242.

MELVILLE, W. K. & HELFRICH, K. R. 1987 Transcritical two-layer flow over topography. *J. Fluid Mech.* **178**, 31–52.

MITSUDERA, H. & GRIMSHAW, R. 1990 Resonant forcing of coastally trapped waves in a continuously stratified ocean. *Pageoph* **133**, 635–644.

PRATT, L. J. & ARMI, L. 1987 Hydraulic control of flows with nonuniform potential vorticity. *J. Phys. Oceanogr.* **17**, 2016–2029.

WARN, T. 1983 The evolution of finite amplitude solitary Rossby waves on a weak shear. *Stud. Appl. Maths.* **69**, 127–133.

WEI, S. N., KAO, T. W. & PAO, H. P. 1975 Experimental study of upstream influence in the two-dimensional flow of a stratified fluid over an obstacle. *Geophys. Fluid Dyn.* **6**, 315–336.

WU, T. Y. 1987 Generation of upstream advancing solitons by moving disturbances. *J. Fluid Mech.* **184**, 75–99.

YI ZENGXIN & WARN, T. 1987 A numerical method for solving the evolution equation of solitary Rossby waves on a weak shear. *Adv. Atmos. Sci.* **4**, 43–54.

YIH, C. S. 1960 Exact solutions for steady two-dimensional flows of a stratified fluid. *J. Fluid Mech.* **9**, 161–174.

ZHU, J. 1986 Internal solitons generated by moving disturbances. PhD thesis, Cal. Inst. Tech., 209 pp.